Mishandling of the Therapeutic Peptide Glucagon Generates Cytotoxic Amyloidogenic Fibrils

Satomi Onoue,[1,2,6,7] Keiichi Ohshima,[3] Kazuhiro Debari,[4] Keitatsu Koh,[4] Seiji Shioda,[5] Sumiko Iwasa,[1] Kazuhisa Kashimoto,[2] and Takehiko Yajima[1]

Received March 8, 2004; accepted March 23, 2004

Purpose. Some therapeutic peptides exhibit amyloidogenic properties that cause insolubility and cytotoxicity against neuronal cells *in vitro*. Here, we characterize the conformational change in monomeric therapeutic peptide to its fibrillar aggregate in order to prevent amyloidogenic formation during clinical application.

Methods. Therapeutic peptides including glucagon, porcine secretin, and salmon calcitonin were dissolved in acidic solution at concentrations ranging from 1 mg/ml to 80 mg/ml and then aged at 37°C. Amyloidogenic properties were assessed by circular dichroism (CD), electron microscopy (EM), staining with β-sheet-specific dyes, and size-exclusion chromatography (SEC). Cytotoxic characteristics were determined concomitantly.

Results. By aging at 2.5 mg/ml or higher for 24 h, monomeric glucagon was converted to fibrillar aggregates consisting of a β-sheet-rich structure with multimeric states of glucagon. Although no aggregation was observed by aging at the clinical concentration of 1 mg/ml for 1 day, 30-day aging resulted in the generation of fibrillar aggregates. The addition of anti-glucagon serum significantly inhibited fibrillar conversion of monomeric glucagon. Glucagon fibrils induced significant cell death and activated an apoptotic enzyme, caspase-3, in PC12 cells and NIH-3T3 cells. Caspase inhibitors attenuated this toxicity in a dose-dependent manner, indicating the involvement of apoptotic signaling pathways in the fibrillar formation of glucagon. On the contrary to glucagon, salmon calcitonin exhibited aggregation at a much higher concentration of 40 mg/ml and secretin showed no aggregation at the concentration as high as 75 mg/ml.

Conclusions. These results indicated that glucagon was self-associated by its β-sheet-rich intermolecular structure during the aging process under concentrated conditions to induce fibrillar aggregates. Glucagon has the same amyloidogenic propensities as pathologically related peptides such as β-amyloid $(A\beta)_{1-42}$ and prion protein fragment $(PrP)_{106-126}$ including conformational change to a β-sheet-rich structure and cytotoxic effects by activating caspases. These findings suggest that inappropriate preparation and application of therapeutic glucagon may cause undesirable insoluble products and side effects such as amyloidosis in clinical application.

KEY WORDS: aggregation; fibril toxicity; glucagon; salmon calcitonin.

INTRODUCTION

Glucagon is a polypeptide hormone that consists of 29 amino acid residues and plays a central role in the maintenance of normal circulating glucose levels (1). The administration of glucagon induces an increase in hepatic glycogenolysis and gluconeogenesis, and attenuates the ability of insulin to inhibit these processes. Glucagon is widely used for peroral endoscopy, clinical diacrisis, and treatment of hypoglycemia. Water-insoluble glucagon is usually solubilized at acidic pH. However, there is at least one serious problem regarding the physicochemical property of glucagon in solution, resulting in glucagon forming gel-like fibrillar aggregates in dilute acid (2). Glucagon is largely unfolded with few stable intramolecular bonds under clinical usage, while the conformation in glucagon fibrils is mainly β-sheet-rich. Other therapeutic peptides such as insulin (3), GLP-1 analog (4), and growth hormone (5) also display conformational changes into β-sheet-rich fibrils. These insoluble products are attributed to the formation of partially unfolded intermediates with an exposed hydrophobic region that drives the aggregation toward the pharmaceutically undesirable form (6).

The generation of insoluble peptide/protein fibrils is well-confirmed in amyloidosis, complex disorders characterized by the polymerization and aggregation of normally innocuous and soluble proteins or peptides followed by extracellular insoluble fibrils with resistance to peptidases (7,8). There are at least 16 proteins forming amyloid fibrils in clinically diverse conditions, which include β-amyloid (Aβ) in Alzheimer's disease (9), amylin in type II (non-insulin-dependent) diabete mellitus (10), prion protein (PrP) in Creutzfeldt-Jakob disease and spongiform encephalopathy (11), and polyglutamine in Huntington's disease (12). These pathologically related amyloidogenic protein/peptide fibrils share a distinct conformational feature in the richness of the β-sheet structure (13). In addition, there are similar characteristics of polarity, hydrophobicity, and the size of side-chain among certain segments containing 10–15 amino acid residues of amyloid-forming peptides such as insulin, Aβ, and amylin, and these factors were indicative of a consensus sequence as a recognition motif of Congo Red, a specific dye for amyloidogenic protein/peptide fibrils with β-sheet dependency (14,15). Because there are similar neurotoxic effects of fibrils from pathologically related peptides and non-pathologically related peptides including glucagon (16), it is plausible that there is also a common toxic mechanism related to their sec-

[1] Department of Analytical Chemistry, Faculty of Pharmaceutical Sciences, Toho University, Funabashi, Chiba 274-8510, Japan.
[2] Health Science Division, Itoham Foods Inc., Moriya, Ibaraki 302-0104, Japan.
[3] Applied Genome Informatics Division, Shizuoka Cancer Center Research Institute, Shizuoka 411-8777, Japan
[4] Laboratory of Electron Microscopy, Showa University School of Medicine, Shinagawa, Tokyo 142-8555, Japan.
[5] Department of Anatomy I, Showa University School of Medicine, Shinagawa, Tokyo 142-8555, Japan.
[6] To whom correspondence should be addressed. (e-mail onoue@fureai.or.jp)
[7] Current address: Pfizer Global Research and Development, Nagoya Laboratories, Pfizer Japan Inc., 5-2 Taketoyo, Aichi 470-2393, Japan. Tel: +81-569-74-4855; Fax: +81-569-74-4748; E-mail: onoue@fureai.or.jp

ABBREVIATIONS: Aβ, amyloid β peptide; PrP, prion protein; WST-8, 4-[3-(2-methoxy-4-nitrophenyl)-2-(4-nitrophenyl)-2*H*-5-tetrazolio]-1, 3-benzene disulfonate sodium salt; Ac-DEVD-CHO, acetyl-Asp-Glu-Val-Asp-1-al; Z-VAD-FMK, *N*-benzyloxycarbonyl-Val-Ala-Asp(O-Me) fluoromethyl ketone; TEM, transmission electron microscopy; CD, circular dichroism; ThT, thioflavin T; SEC, size-exclusion chromatography; DMEM, Dulbecco's modified Eagle's medium; LDH, lactate dehydrogenase.

0724-8741/04/0700-1274/0 © 2004 Plenum Publishing Corporation

ondary and macromolecular structures for different amyloid-forming proteins/peptides.

In this investigation, we have characterized the physicochemical and physiological properties of glucagon fibrils using biophysical techniques including circular dichroism (CD), transmission electron microscopy (TEM), β-sheet-imaging probes, and size-exclusion chromatography (SEC). As well as glucagon, we also investigated the characteristics of other therapeutic peptides, which include porcine secretin that exhibits 52% amino acid sequence homology to glucagon (17) and salmon calcitonin, a therapeutic peptide used for the treatment of osteoporosis, Paget's disease, and hypercalcemia (18). We have demonstrated that glucagon requires the lowest concentration for fibril formation among those three therapeutic peptides and the peptide fibrils of glucagon and salmon calcitonin possess the same conformational properties and cytotoxic apoptotic signaling pathways by activating caspases as fibrils derived from pathologically-related peptides including $A\beta_{1-42}$ and $PrP_{106-126}$. Here, we provide further insights into the associative behavior of glucagon, showing that its noncovalent aggregation was dependent on the condition for storage.

MATERIALS AND METHODS

Chemicals

Human glucagon and porcine secretin were synthesized by the solid-phase strategy employing optimal side-chain protection as reported previously (19). Salmon calcitonin, $A\beta_{1-42}$ and $PrP_{106-126}$ were purchased from American Peptide Company (Sunnyvale, CA, USA). Congo Red and thioflavin T (ThT) were purchased from Wako (Osaka, Japan), and WST-8 [2-(2-methoxy-4-nitrophenyl)-3-(4-nitrophenyl)-5-(2,4-disulfophenyl)-2H-tetrazolium, monosodium salt] was obtained from Dojindo (Kumamoto, Japan). Ac-DEVD-CHO and Z-VAD-FMK, caspase inhibitors, were purchased from Promega (Madison, WI, USA). Calibration standards for size-exclusion column chromatography (SEC) were obtained from Sigma (St. Louis, MO, USA). Human glucagon antibody YP040 was obtained from Yanaihara Institute, Inc. (Fujinomiya, Japan).

Aging Treatment of Peptides

Glucagon, salmon calcitonin, and porcine secretin were dissolved in 0.01 M HCl at the concentration indicated in the text. $A\beta_{1-42}$ and $PrP_{106-126}$ were prepared in sterile water as 5 and 10 mg/ml stocks, respectively (20,21). Peptides were incubated at 37°C for the periods indicated in the text and then diluted to the required concentration.

Transmission Electron Microscopy

An aliquot (2 μl) of the peptide gels or solution was placed on a carbon-coated Formvar 200 mesh nickel grid. The sample was allowed to stand for 15–30 s, and then any excess solution was removed by blotting. The samples were negatively stained with 2% (w/v) uranyl acetate and allowed to dry. The samples were then visualized under a Hitachi H-7000 transmission electron microscope operating at 75 kV. The magnification ranged from ×12,000 to ×60,000.

Circular Dichroism Analysis of Amyloidogenic Peptides

Aged preparations of peptides were dissolved in 20 mM Tris-HCl buffer (pH 7.4) or 50% methanol (MeOH)/20 mM Tris-HCl buffer, and circular dichroism (CD) spectra (average of ten scans) were collected from samples (2 ml) at 0.5 nm intervals between wavelengths of 200 and 400 nm using a Jasco model J-720 spectropolarimeter (Tokyo, Japan). Samples were incubated at room temperature and a baseline spectrum was subtracted from the collected data.

Congo Red Binding Assay

Congo Red-reactive fibrils were measured as described previously (22). Aged preparations of peptides were adjusted to a concentration of 1 mg/ml, and 40 μl of each dilution was added to 960 μl of 25 μM Congo Red in 20 mM potassium phosphate buffer (PBS, pH 7.4) containing 150 mM NaCl. After a 30-min incubation, absorbance was read at 540 and 477 nm, and the concentration of bound Congo Red (c_b) was calculated from the equation, $c_b = (A540/25{,}295 - A477/46{,}306)$.

Thioflavin T Binding Assay

Formation of peptide fibrils was fluorimetrically quantified by thioflavin T (ThT) binding (23). An aliquot of 20 μl of each aged preparation was added to 1980 μl of 5 μM ThT in 20 mM PBS (pH 6.0) containing 150 mM NaCl. Fluorescence was immediately measured on an RF-5000 spectrofluorophotometer (Shimadzu, Tokyo, Japan) with excitation and emission maxima of 450 and 482 nm, respectively.

Turbidity

Glucagon was aged at concentrations of 1.0, 2.5, or 5.0 mg/ml for 24 h in 0.01 M HCl. For turbidity analysis, samples aged at the concentrations of 2.5 and 5.0 mg/ml were diluted to a final concentration of 1 mg/ml with 0.01 M HCl. An aliquot of 200 μl of each aged sample as well as non-aged glucagon (1.0 mg/ml) was transferred into a 96-well plate and turbidity (OD) was measured at 405 nm with a microplate reader (Bio-Tek, Winooski, VT, USA).

Size-Exclusion Chromatography

Aged preparations of peptides were fractionated on a Zorbax GF-250 column (Agilent Technologies, Palo Alto, CA, USA) at 25°C using a Shimadzu LC-10A HPLC system. The column was equilibrated with the mobile phase (20 mM citrate buffer containing 130 mM NaCl, pH 3.0), and peptides were eluted under constant flow at 1.0 ml/min and monitored at 220 nm. The column was calibrated with blue dextran (2,000,000 Da) and a series of molecular weight protein standards including, sweet potato β-amylase (200,000 Da), human serum albumin (66,500 Da), chicken albumin (45,000 Da), human growth hormone (22,125 Da), porcine insulin (5,777 Da), and buserelin (1239 Da).

Cell Cultures

Rat pheochromocytoma (PC12) cells were obtained from the RIKEN Cell Bank (Ibaraki, Japan). PC12 cells were cultured in Dulbecco's modified Eagle's medium (DMEM, Sigma) supplemented with 5% (v/v) horse serum (HS, Gibco-BRL, Grand Island, NY, USA) and 5% (v/v) newborn calf serum (CS, Gibco-BRL) as described previously (24). NIH-3T3 cells were purchased from American Type Culture Collection (Manassas, VA, USA) and cultured in DMEM supple-

mented with 10% CS. Cells were maintained in 5% CO_2/95% humidified air at 37°C.

LDH and WST-8 Assay

Cells were seeded at 1×10^4 cells/well in 96-well plates coated with type I collagen (Becton Dickinson Labware, Bedford, MA, USA) at least 24 h before the experiment and cultured in serum-free DMEM supplemented with 2 μM insulin. For preparation of peptide fibrils, therapeutic peptides, glucagon and salmon calcitonin, were incubated for 24 h at 5.0 mg/ml and at 60 mg/ml, respectively, and their fibril production was assessed by the Congo Red binding assay. Each aged or nontreated peptide was diluted and added to the cell culture at the indicated final concentrations. The degree of cell death was assessed by measurement of the activity of lactate dehydrogenase (LDH) released from the dead cells as reported previously (20). LDH activity in the culture medium was determined using a commercially available kit (Wako, Osaka, Japan) according to the manufacturer's protocol. In addition to LDH measurement in the medium, cell mortality was also assayed by WST-8 conversion (25). A volume of 10 μl of WST-8 (5 mM WST-8, 0.2 mM 1-methoxy-5-methylphenazinium methylsulfate, and 150 mM NaCl) was added to each well and the reaction was continued for 4 h at 37°C. The absorbance of the sample at 450 nm was measured using a microplate reader (Bio-Tek) with a reference wavelength of 720 nm.

Caspase-3-like Activity

Caspase-3-like activity in culture was measured using an Apo-ONE Homogeneous Caspase-3/7 Assay Kit (Promega) according to the manufacturer's instructions. Briefly, cells (5×10^4 cells/well) in type I collagen-coated 96-well plates (Becton Dickinson Labware) were rinsed twice with PBS. The cultures were incubated with or without the indicated stimulators in DMEM (50 μl) at 37°C in an atmosphere of 95% air and 5% CO_2. The cells were lysed in 50 μl of Homogeneous Caspase-3/7 Buffer containing the caspase-3 substrate Z-DEVD-Rhodamine 110, and the cell lysates were incubated for 12 h at room temperature. After incubation, the fluorescence (excitation 480 nm and emission 535 nm) of the cell lysates (50 μl) was measured with a GEMINIxs spectrofluorophotometer (Molecular Devices, Kobe, Japan).

Statistical Analysis

Statistical evaluation was performed by the Student's *t* test or one-way analysis of variance (ANOVA) along with pairwise comparison by the Fisher's least significant difference procedure. p values less than 0.05 were considered to be significant in all analyses.

RESULTS

CD Spectral Analyses on Aged Peptides

CD is displayed when an optically active substance preferentially absorbs left or right-handed circularly polarized light and it provides useful information when conformational alterations occur in peptides/proteins (26). The CD spectrum of a β-sheet structure shows an intense positive band at 198 nm and a negative extremal band at 218 nm (27), and the CD spectrum of α-helical structure shows an intense positive peak at 192 nm and two negative peaks at 209 nm and 222 nm (26). The well-known amyloidogenic peptides, $PrP_{106–126}$ and $A\beta_{1–42}$, gave typical CD spectra for the presence of a β-sheet structure after aging under both hydrophilic (20 mM Tris-HCl buffer, pH 7.4) and hydrophobic (50% MeOH/20 mM Tris-HCl buffer, pH 7.4) conditions (Figs. 1D and 1E). When glucagon was dissolved in the hydrophilic buffer at 10 mg/ml, non-aged glucagon gave the characteristic CD spectrum of a random coil conformation (Figs. 1A-I). However, when glucagon was aged for 24 h, a transition from random coil to β-sheet structure was observed for preparations dissolved at 5 mg/ml or higher. In the hydrophobic condition, the CD spectra of non-aged glucagon exhibited a typical α-helical structure (Fig. 1A-II), the content of which was estimated to be 55% according to the calculation established by Greenfield&Fasman (26). When aged at 1 mg/ml for 24 h, the α-helical content of glucagon was not changed, whereas aging at 2.5 mg/ml or higher resulted in a significant decrease in the α-helical content to ca. 1%.

We also tested the effect of aging and concentration on the conformational change for other therapeutic peptides, porcine secretin and salmon calcitonin. Porcine secretin has high sequential homology to glucagon and the CD spectra of both non-aged peptides exhibited high similarity (Figs. 1A and 1B). On the contrary to glucagon, the CD spectrum of aged secretin at the concentration of 75 mg/ml was almost identical to that of non-aged secretin (Figs. 1B-I and 1B-II), suggesting no conformational changes to peptide aggregate of β-sheet-rich structures. Salmon calcitonin, without aging at concentrations as high as 75 mg/ml or with aging at a low concentration of 1 mg/ml, showed the presence of a random coil structure in the hydrophilic environment (Fig. 1C-I) and a typical α-helical structure in the hydrophobic environment (Fig. 1C-II). However, as in the case of glucagon, a conformational transition from an α-helical structure to β-sheet structure was observed after aging at high concentrations of 50 and 75 mg/ml (Fig. 1C). It was thus shown that salmon calcitonin requires about a 10-fold higher concentration than glucagon for structural changes to occur, suggesting that glucagon has a high propensity to yield β-sheet structure.

Electron Microscopic Studies on Peptide Aggregates

Initially, human glucagon was incubated at a concentration of 10 mg/ml in 0.01 M HCl for 24 h at 37°C and diluted to a final concentration of 1.0 mg/ml prior to applying on transmission electron microscopy (TEM). TEM showed well-defined fibrils (Fig. 2A), which morphologically resembled the classic amyloid fibrils such as $A\beta_{1–42}$ and $PrP_{106–126}$ (28,29). The fibril morphologies included largely disordered, rigid, and branching fibrils stacked together edge to edge with a width of 10–50 nm and various lengths. Similar fibril structures were observed for salmon calcitonin aged at the concentration of 60 mg/ml for 24 h (Fig. 2B).

Physicochemical Properties of Peptide Aggregates

TEM analysis and CD spectral analyses on aged and concentrated glucagon and salmon calcitonin revealed the presence of amyloidogenic fibrils and conformational alterations

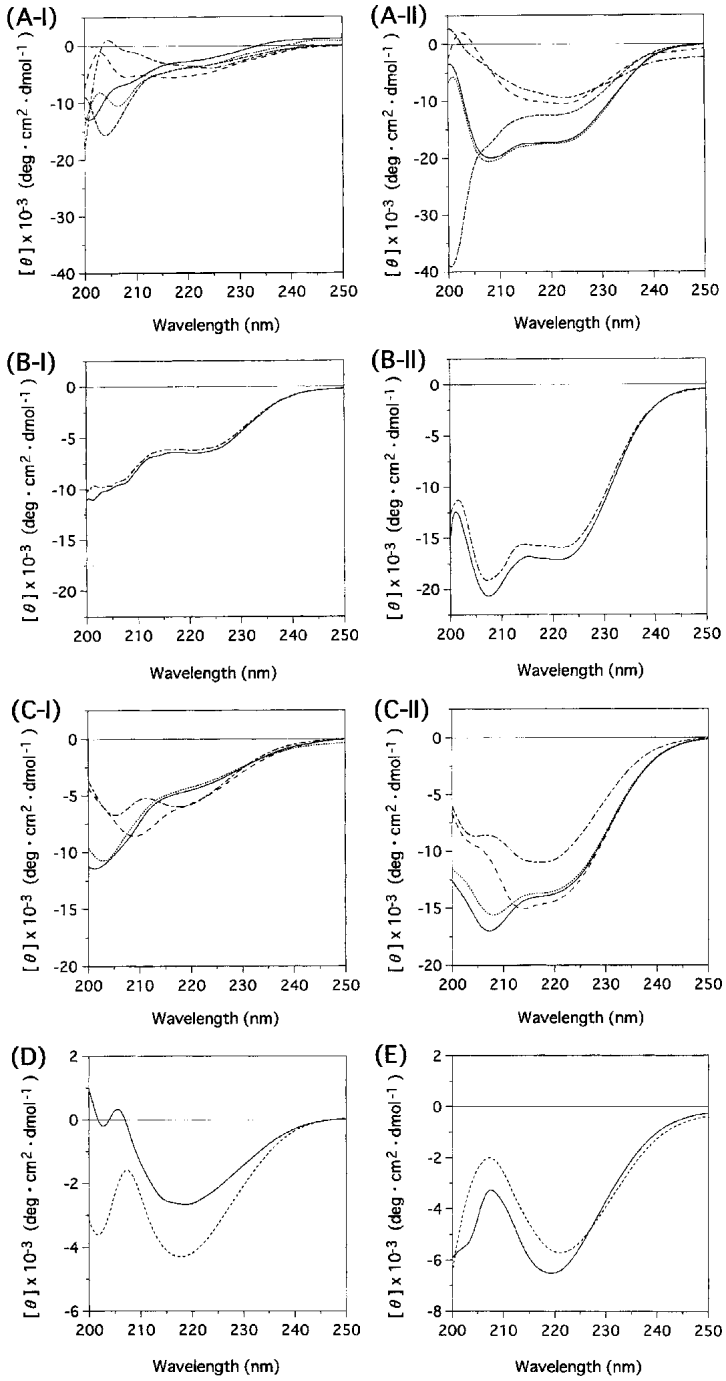

Fig. 1. CD spectra representative of glucagon, salmon calcitonin, $PrP_{106–126}$, and $A\beta_{1–42}$. (A) CD spectra of non-aged or aged glucagon in 20 mM Tris-HCl buffer, pH 7.4 (A-I) or 50% MeOH/20 mM Tris-HCl buffer, pH 7.4 (A-II). Solid line, non-aged glucagon; dotted line, glucagon aged at 1 mg/ml; dashed line, aged at 2.5 mg/ml; broken line, aged at 5 mg/ml; and chain line, aged at 10 mg/ml. (B) CD spectra of non-aged or aged secretin in 20mM Tris-HCl buffer, pH 7.4 (B-I) or 50% MeOH/20 mM Tris-HCl buffer, pH 7.4 (B-II). Solid line, non-aged porcine secretin; and chain line, aged at 75 mg/ml. (C) CD spectra of non-aged or aged salmon calcitoin in 20mM Tris-HCl buffer, pH 7.4 (C-I) or 50% MeOH/20 mM Tris-HCl buffer, pH 7.4 (C-II). Solid line, non-aged salmon calcitonin; dotted line, salmon calcitoin aged at 1 mg/ml; dashed line, aged at 50 mg/ml; and chain line, aged at 75 mg/ml. (D) CD spectra of non-aged or aged $PrP_{106–126}$ in 20 mM Tris-HCl buffer, pH 7.4 (solid line) or 50% MeOH/20 mM Tris-HCl buffer, pH 7.4 (dashed line). (E) CD spectra of normal or aged $A\beta_{1–42}$ in 20 mM Tris-HCl buffer, pH 7.4 (solid line) or 50% MeOH/20 mM Tris-HCl buffer, pH 7.4 (dashed line).

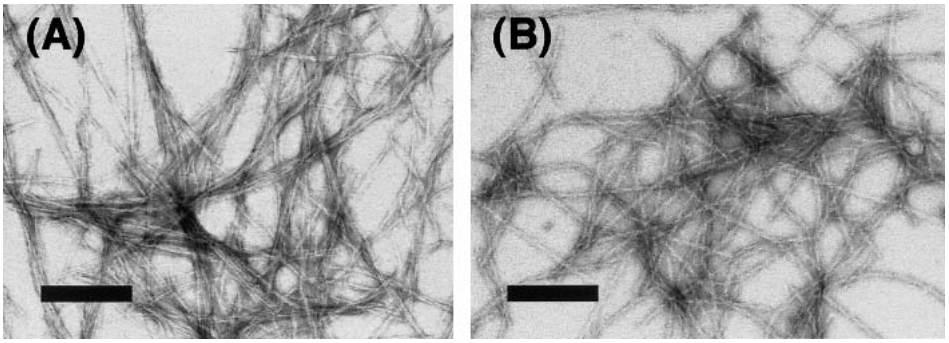

Fig. 2. Electron micrographs of negatively stained fibrils formed by aged (A) glucagon and (B) salmon calcitonin. Fibrils of glucagon and salmon calcitonin were prepared by aging at the concentration of 10 and 60 mg/ml, respectively, in 0.01 M HCl for 24 h. Prior to TEM analysis, the samples were diluted to the final concentration of 1 mg/ml. The bars represent 0.2 μm.

to the β-sheet structures, respectively. Here, in order to put these observations together, we performed physicochemical analyses including the binding assay using Congo Red and ThT, and turbidity assays. Congo Red selectively binds to amyloid-like aggregates having a β-sheet rich conformation, and is used to detect amyloid fibrils in pathological specimens (30). When glucagon was incubated at various concentrations ranging from 1 to 10 mg/ml at 37°C, bathochromic effect was observed upon staining with Congo Red, indicating the formation of aggregate at 5 mg/ml or higher (Fig. 3A). The rate of aggregation was in a time-dependent manner; it reached the maximal level approximately 6 min after aging at 7.5 and 10 mg/ml and 25 min at 5 mg/ml. Glucagon at 1 and 2.5 mg/ml did not show any signs of fibrillar formation within 24 h aging.

In addition to Congo Red, ThT has also been used commonly as an amyloid-binding dye for *in vitro* studies (23), and this fluorochrome is considered to be a potential pharmacophore for further design of amyloid-imaging agents. ThT binding activities were observed in the glucagon preparations aged at 2.5 and 5 mg/ml for 24 h, and their fluorescence intensities at each concentration were 5-fold and 20-fold higher than those of glucagon with or without aging at 1 mg/ml, respectively (Fig. 3B). There was also a significant increase in the turbidity 24 h in the glucagon preparation aged at 2.5 and 5 mg/ml for 24 h, whereas the turbidity of the preparation aged at 1 mg/ml was almost equal to that of the non-aged preparation at 1 mg/ml (Fig. 3C). Hence, these physicochemical analyses indicated that aging at higher concentrations (>5 mg/ml) accelerated the misfolding of glucagon, producing amyloidogenic fibrils readily.

Surprisingly, when glucagon was aged at 1 mg/ml for 30 days at room temperature, the presence of a β-sheet structure was detected by both Congo Red and ThT binding analyses (data not shown). It should also be pointed out that a concomitant formation of a fibrillar aggregate was observed in TEM analysis (data not shown).

The physicochemical properties on salmon calcitonin are summarized in Table I. Peptide aggregation was indicated by the increases in turbidity, Congo Red and ThT bindings after 24 h aging. The peptide concentration requisite for aggregation was 40 mg/ml in turbidity and ThT binding analyses and 60 mg/ml in Congo Red binding analysis, which was almost consistent with the result of the CD study.

Size-Exclusion Chromatography of Glucagon Aggregate

We performed size exclusion chromatography (SEC) to check the size and molecular pattern of the glucagon aggregate. Each glucagon preparation aged for 0, 1, 3, and 6 h was applied to a SEC column (ZORBAX Bio Series GF-250) at 7.5 mg/ml. The SEC analysis performed with 20 mM sodium phosphate buffer containing 130 mM NaCl (pH 7.4) revealed that there was only one peak at 3.5 kDa corresponding to a molecular weight of monomeric glucagon even with the preparations of glucagon aggregate or non-aged glucagon, suggesting that the aggregated glucagon was immediately disaggregated on SEC. On the other hand, when 20 mM citrate-HCl buffer containing 130 mM NaCl (pH 3.0) was used as the mobile phase, a main peak appeared at 2000 kDa for the glucagon aggregate (Fig. 4A), suggesting that glucagon fibril was much stable in the acidic condition as compared to the neutral condition. During the time course from the non-aging state to 6 h aging, the peak at 3.5 kDa of monomeric glucagon was shifted to generate a peak at 2000 kDa, suggesting that intermolecular association is likely to be involved in the generation of the glucagon aggregate.

Under the acidic condition, the retention times for molecular weight standards and non-aged glucagon were well associated with each molecular weight (MW) in the range from 1.2 kDa to 2000 kDa. The correlation coefficient between retention time and Mw was estimated to be $r^2 = 0.95$ ($p < 0.01$) according to the log(MW) vs. elution time standard curve (Fig. 4B).

Inhibition of Glucagon Antiserum on the Formation of Glucagon Aggregate

The antisera raised against $A\beta_{1-42}$, $PrP_{106-126}$, and polyglutamine have the ability to suppress their respective aggregations *in vitro* and *in vivo* (29,31,32). Thus, we examined the effect of antiserum against glucagon on the formation of glucagon fibrils. According to X-ray analysis, glucagon adopts a mainly α-helical conformation in the amino acid sequence between positions 10 and 25, which is stabilized by the hydrophobic interactions between glucagon molecules related by 3-fold symmetry (33). The glucagon antiserum used recognized the entire glucagon molecule but not a fragment of $glucagon_{1-12}$ (data not shown), indicating that the α-helical

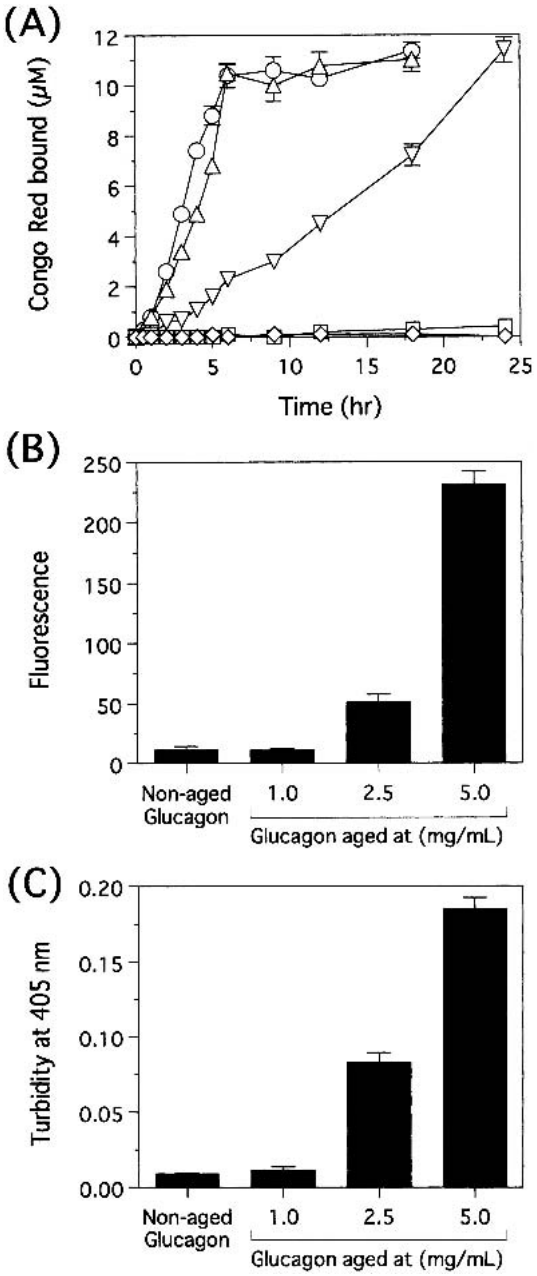

Fig. 3. Physicochemical analyses of glucagon on the formation of amyloid fibrils. (A) Time course of glucagon aggregation as monitored by Congo Red binding assay. Glucagon was incubated at various concentrations (◇, 1.0 mg/ml; □, 2.5 mg/ml; ▽, 5.0 mg/ml; △, 7.5 mg/ml; ○, 10 mg/ml) in 20 mM NaPB (pH 7.4) at 37°C for various time periods up to 24 h. Samples aged at the concentrations higher than 1 mg/ml were adjusted to 1 mg/ml with 0.01 M HCl and applied to Congo Red binding assay as described in "Materials and Methods." (B) ThT binding assay. Glucagon was aged at the concentration of 1.0, 2.5, or 5.0 mg/ml for 24 h in 0.01 M HCl. Samples aged at the concentration of 2.5 and 5.0 mg/ml were diluted to the final concentration of 1 mg/ml with 0.01 M HCl. Binding abilities of ThT against non-aged (1.0 mg/ml) and aged glucagon were measured as described in "Materials and Methods." (C) Turbidity assay: Glucagon was aged at the concentration of 1.0, 2.5, or 5.0 mg/ml for 24 h in 0.01 M HCl. Samples aged at the concentration of 2.5 and 5.0 mg/ml were diluted to the final concentration of 1 mg/ml with 0.01 M HCl. Turbidities of non-aged (1.0 mg/ml) and aged glucagon were measured at OD 405 nm as described in "Materials and Methods." Each point represents the mean ± SD of four determinations.

Table I. Physicochemical Analyses of Aged Salmon Calcitonin

Aging concentration (mg/ml)	Misfolding properties		
	Turbidity at 405 nm (% of control)	Bound Congo Red (Δ μM)	Thioflavin T fluoresecence (% of control)
20.0	100 ± 09	0	100 ± 04
40.0	154 ± 16	0.3	351 ± 13
60.0	355 ± 46	9.9 ± 1.2	665 ± 34
80.0	464 ± 42	11.5 ± 1.0	713 ± 56

Salmon calcitonin was dissolved in 20 mM PBS (pH 7.4) containing 150 mM NaCl at the concentrations of 20, 40, 60, and 80 mg/ml and aged for 24 h at 37°C. Misfolding properties of salmon calcitonin were assessed by turbidity, Congo Red staining, and ThT fluorometric assays. Data represent the mean ± SD of four experiments.

region in the C-terminal moiety of glucagon represents the epitope of this antiserum. When the glucagon antiserum was added at the dilution of 1:20 or 1:50 to glucagon dissolved at 5 mg/ml and aged at 37°C for 24 h, it decreased the fibrillar formation of glucagon by 70% and 50%, respectively, as measured by Congo Red binding assay (Fig. 5) as well as ThT binding fluorescence assay (data not shown). The addition of unrelated control serum had no effect on fibril formation.

Cytotoxicity of Peptide Fibrils

To assess the cytotoxicity of the glucagon fibrils, PC12 cells and NIH-3T3 cells were exposed to 0.1–100 μM peptide aggregate for 72 h followed by the measurement of cell viability determined by WST-8 assay and released LDH. A significant decrease in cell viability was observed in cultures exposed to 10–100 μM aged glucagon ($p < 0.01$) but not in cultures treated with 100 μM non-aged glucagon (Fig. 6A, hatched bars). To determine whether the loss of cell viability was equivalent to cell death, the release of LDH was measured. Treatment with 10 μM aged glucagon induced a significant increase in LDH release compared to control and no significant increase in LDH release was observed in cultures treated with non-aged glucagon at 100 μM and aged glucagon at 1 μM or lower (data not shown). Thus, glucagon fibrils were found to be highly toxic to PC12 cells, which was similar to the case of aged $PrP_{106–126}$ and $A\beta_{1–42}$ (>10 μM) (20,21). Aged salmon calcitonin also displayed significant cytotoxicity in PC12 cells (Fig. 6A, filled bars), whereas non-aged salmon calcitonin did not induce significant cell death. As shown in Fig. 6B, the incubation of NIH-3T3 cells with these peptide fibrils at 25 μM or higher for 48 h resulted in a significant decrease in cell viability. On the contrary, non-aged peptides were not toxic to NIH-3T3 cells. These findings suggested that the presence of amyloid fibrils was responsible for the cytotoxicity of aged glucagon or aged salmon calcitonin toward both PC12 cells and NIH-3T3 cells. These results were consistent with a previous report showing that peptide fibrils induced neurotoxicity in cultured hippocampal neurons while native peptide did not affect the cell survival as measured by MTT assay (34).

Signaling Pathways in the Cytotoxicity of Peptide Fibrils

Caspases, a family of cysteine proteases, are key mediators of apoptosis. In particular, the activation of caspase-3 is

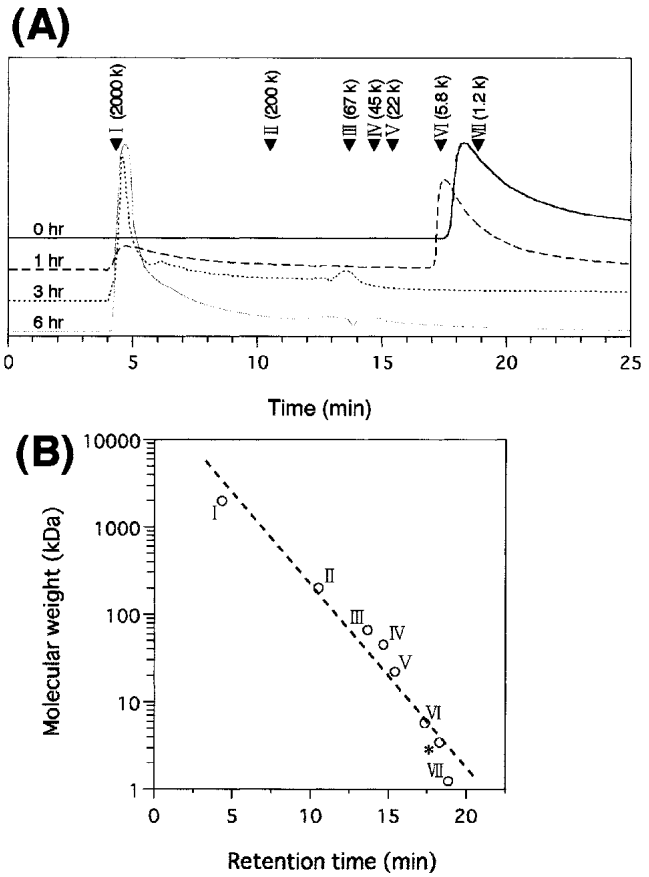

Fig. 4. Size-exclusion chromatography of aged glucagon. (A) The elution profile of aged glucagon on a Zorbax GF-250 size exclusion column. Glucagon was incubated at the concentration of 7.5 mg/ml at 37°C. Each sample aged at the periods of 0, 1, 3, and 6 h was applied on SEC. Arrows (I–VII) represent elutions of a series of the following molecular weight protein standards with their retention times: I, blue dextran (2000 kDa); II, sweet potato β-amylase (200 kDa); III, human serum albumin (66.5 kDa): IV, chicken albumin (45 kDa); V, human growth hormone (22.1 kDa); VI, porcine insulin (5.8 kDa); VII, buserelin (1.2 kDa); and *, glucagon (3.5 kDa). Samples were loaded on a SEC column in 20 mM citrate buffer (pH 3.0), and the elution profiles were determined by UV detection at 280 nm. (B) Standard curve of the log (Mw) vs. elution times.

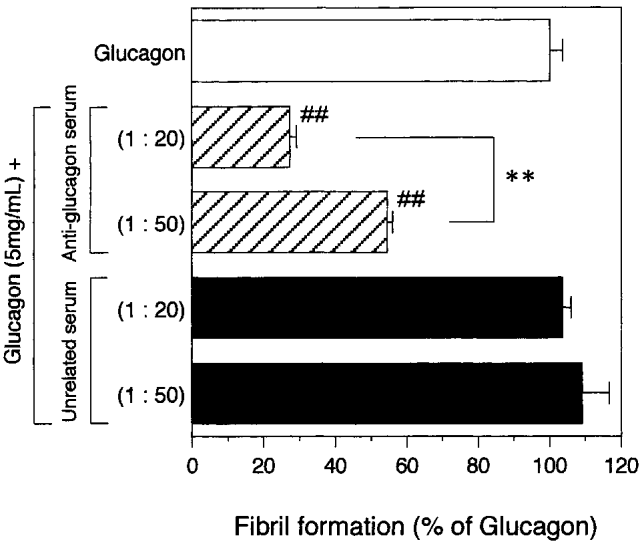

Fig. 5. Effect of glucagon antiserum on the fibril formation of glucagon. Glucagon was dissolved in 0.01 M HCl, and then glucagon antiserum or unrelated antiserum was immediately added. The mixture was incubated for 24 h at 37°C. In the mixture, the final concentration of glucagon was 5.0 mg/ml. The molar ratio between serum (anti-glucagon antiserum, hatched bars; unrelated serum, filled bars) and the peptide was 1: 20 and 1: 50. Fibril formation was assessed by the Congo Red-binding assay. All data are scaled with glucagon alone representing 100% aggregation, and data represent the mean ± SD of four determinations. $^{\#\#}p < 0.01$ with respect to the control group (glucagon alone). $^{**}p < 0.01$ between indicated groups.

required for the early stages of apoptosis that include DNA fragmentation and morphological changes (35). To determine whether aged glucagon induces caspase-3 activation in PC12 cells, we exposed PC12 cells to the aged peptide (50 μM) and measured caspase-3-like activity in cell lysates obtained by the cleavage of a fluorometric caspase-3 substrate, Z-DEVD-Rhodamine 110 (34). The caspase-3 activity increased prior to the loss of membrane integrity, and 24 h after incubation the maximal caspase-3 activity was detected at 160% of the control level (Fig. 7A). On the contrary, no significant elevation of caspase-3 activity was observed in cells treated with non-aged glucagon (50 μM). These data indicated that the exposure of PC12 cells to the peptide fibrils induced a rapid and significant elevation in caspase-3 activity within 24 h prior to the loss of cell viability that occurred 72 h after exposure.

Inhibitors of caspases including Ac-DEVD-CHO, a caspase-3-specific inhibitor (36), and Z-VAD-FMK, an irreversible inhibitor of several members of the caspase family (37), were used to investigate whether apoptosis was involved in the cytotoxicity by aged glucagon. The addition of Z-VAD-FMK (100 μM) rescued glucagon-induced cell death close to the control level (vehicle only) and this protective effect was reduced to half at 50 μM (Fig. 7B). On the other hand, Ac-DEVD-CHO attenuated the fibril toxicity by 40% only at high concentration (100 μM). These data indicate that not only caspase-3 but also other caspases may play an important role in the final execution of the cell death program stimulated by aged glucagon.

DISCUSSION

The non-covalent aggregation of pharmaceutical peptides including insulin and glucagon is a well-recognized problem that has been studied largely with regard to insoluble forms (4,38). The glucagon injection is usually prepared just prior to administration by dissolving lyophilized glucagon with distilled water to the concentration of 1 mg/ml. In this study, we demonstrated that concentrated (>2.5 mg/ml) glucagon molecules were converted to fibrillar aggregates within 24 h after being solubilized and kept at 37°C, and glucagon requires the lowest concentration for aggregation among three therapeutic peptides investigated. At 1 mg/ml, no amyloidogenic materials were detected in the glucagon solution when prepared as instructed. However, when the solution was kept at room temperature for a month, most of the glucagon molecules were converted to fibrillar aggregates (data not shown). Thus, it is a matter of concern that fibrillar formation

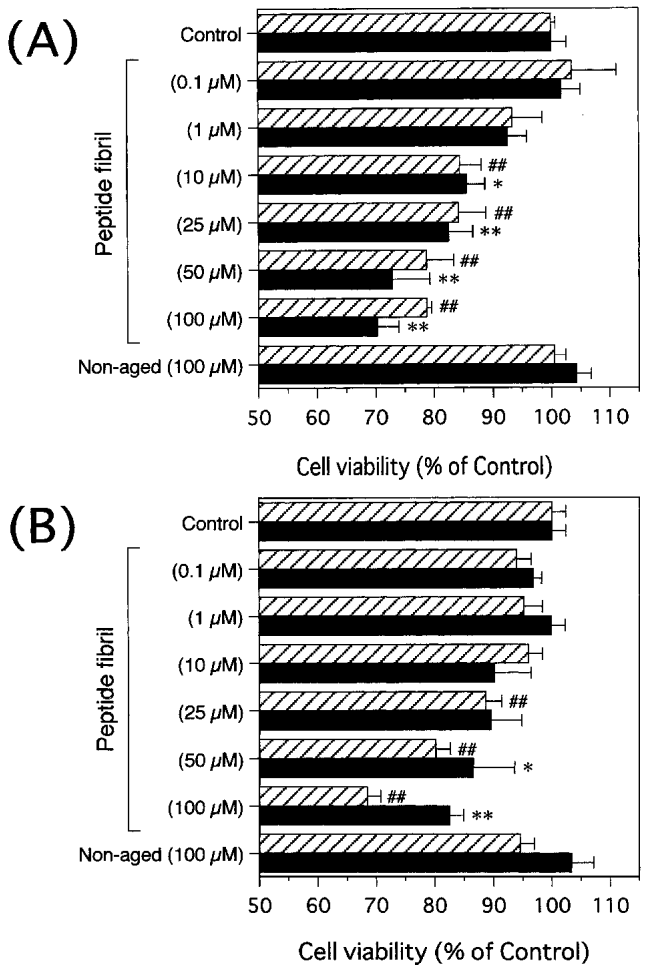

Fig. 6. Effects of aged glucagon and salmon calcitonin on cell viability. (A) PC12 cells and (B) NIH-3T3 cells were treated with different concentrations of non-aged or aged glucagon (hatched bars) and salmon calcitonin (filled bars) for 72 h and 48 h, respectively. After incubation for the defined period, cell viability was determined using WST-8 assay. Data represent the mean ± SD of six determinations. $^{\#\#}p < 0.01$ with respect to the control group (glucagon). $^{**}p < 0.01$ and $^{*}p < 0.05$ with respect to the control group (salmon calcitonin).

may occur in the glucagon injection when prepared by inappropriate procedures such as dissolving glucagon with an insufficient volume of water for extended period of storage before administration.

Salmon calcitonin is used for the treatment of osteoporosis and Paget's disease in lieu of human calcitonin because of its solubility. The concentration of the salmon calcitonin preparation is 5–10 μg/ml. Aggregation of salmon calcitonin occurred when aged at 40 mg/ml, which is much higher than the concentration for clinical use, suggesting that it is unlikely that fibrillar aggregates are produced in the salmon calcitonin preparation. As for porcine secretin, despite of similar CD structural spectrum of α-helix and sequential homology to glucagon, no transition of CD spectrum was observed after aging. According to X-ray crystal analysis, it is likely that amyloid-forming peptides that exhibit interaction of α-helical molecules to change to β-sheet-rich molecules may be enhanced by interaction of aromatic amino acid residues (manuscript in preparation).

The structural transition from α-helix to β-sheet is the main conformational characteristic in the aggregation process of amyloidogenic peptides/proteins including $A\beta_{1-42}$ (39), PrP (40), human amylin (27), GLP-1 analog (4), and human calcitonin (41). Despite having no sequential homology, these aggregated forms share similar ultrastructural and physicochemical properties regarding the richness of the β-sheet conformation. In this study, it was shown that the concentrated and aged glucagon possessed the same amyloidogenic conformational properties of β-sheet transition as $A\beta_{1-42}$ and $PrP_{106-126}$ by electron microscopic and CD spectral analyses, binding assays with Congo Red and ThT, and SEC analysis. In the high polar and/or acidic media, the hydrophobic side groups of amyloidogenic peptides partially tend to huddle together to avoid the aqueous environment (33). However, under highly concentrated conditions, there are hydrophobic interactions within their respective α-helical regions to initiate aggregation. Thus, concentrated and aged glucagon molecules also seem to be self-associated to form highly ordered fibrillar aggregates with β-sheet structures. In addition, we showed that aggregation of glucagon was inhibited by the addition of an anti-glucagon serum, in which the epitope was its C-terminal α-helix forming region. This finding supports the concept that the α-helix region is involved in the aggregation of glucagon.

The family of caspase enzymes is a large group of proteases whose members have defined roles in apoptotic cell death. Among them, the activation of caspase-3 has been linked to the apoptosis induced by many neurotoxic agents including nitric oxide (42), tumor necrosis factor-α, and cycloheximide (43). We showed that fibrillar glucagon and salmon calcitonin caused cytotoxic effects with the activation of caspase-3 in PC12 cells and NIH-3T3 cells. Previous investigation have shown similar cytotoxic mechanisms in fibrillar aggregates derived from various pathologically-related peptides including $A\beta_{1-42}$ and $PrP_{106-126}$ (20,21) and pathologically related peptides/proteins (6–8). Thus, our current study on glucagon provides further evidence for the concept that there is an intrinsic cytotoxic signaling pathway in fibrillar aggregates from various peptides/proteins, suggesting that this cytotoxic mechanism occurs in a conformation-specific manner rather than a sequence-specific manner.

In conclusion, we demonstrated that the misfolding of therapeutic peptide glucagon generated amyloidogenic fibrils, leading to cytotoxicity mediated by activation of the apoptotic enzyme caspase-3 *in vitro*, which is the same cytotoxic property as fibrils from pathologically related peptides including $A\beta_{1-42}$ and $PrP_{106-126}$. This structural transition was accelerated when glucagon solution was prepared at high concentrations (>2.5 mg/ml). At the clinical concentration of 1 mg/ml, no amyloidogenic materials were detected in the glucagon solution prepared as instructed. However, fibrilization could occurr even at 1 mg/ml due to long storage. Therefore, we strongly emphasize that the instructions supplied by manufacturers should be followed strictly. The conformational analyses including staining with specific dyes for β-sheet structures and SEC analysis could be a useful tool for monitoring the process of glucagon aggregation prior to clinical application in order to avoid undesirable side effects in peroral endoscopy, clinical treatment of hypoglycemia, and the clinical diacrisis for insulinoma, growth hormone deficiency, and hepatic glycogenosis.

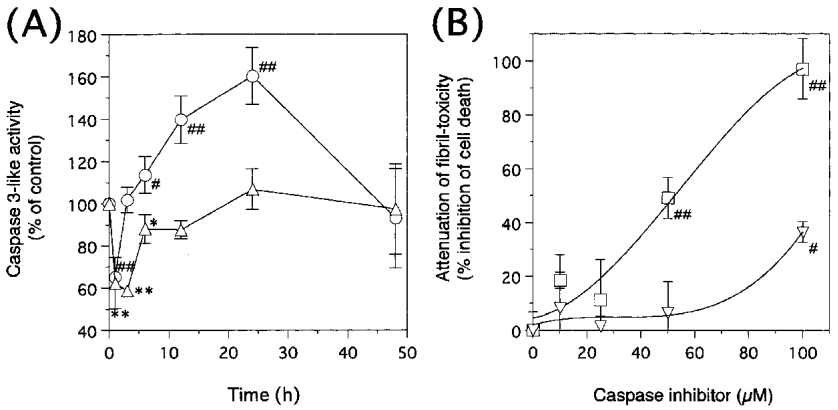

Fig. 7. Involvement of the caspase-3 signaling pathway in the cytotoxic process induced by aged glucagon. (A) Time course of caspase-3 activity in cytosolic protein extracts from PC12 cells treated with non-aged (△) or aged (○) glucagon. PC12 cells were exposed to non-aged or aged glucagon (50 μM) and lysed for the indicated period. Caspase-3-like protease activity was determined by the cleavage of the fluorometrical caspase-3 substrate, Z-DEVD-Rhodamine 110. The data are expressed as percentage of the control value (mean ± SD of four experiments). $^{\#\#}p < 0.01$ and $^{\#}p < 0.05$ between control and aged glucagon-treated group. $^{**}p < 0.01$ and $^{*}p < 0.05$ between control and normal glucagon-treated group. (B) Effects of caspase inhibitors on the cytotoxicity induced by aged glucagon. PC12 cells were chronically treated with 50 μM of aged glucagon for 72 h in the presence of Ac-DEVD-CHO (▽) or Z-VAD-FMK (□) at various concentrations. Cell viability was determined by WST-8 assay. $^{\#\#}p < 0.01$ and $^{\#}p < 0.05$ with respect to the aged glucagon-treated group.

ACKNOWLEDGMENTS

We wish to thank Hajime Sukigara, Yoshimi Itoh, and Shin'ichi Hashimoto, Department of Analytical Chemistry, Faculty of Pharmaceutical Sciences, Toho University, for their excellent technical assistance throughout this work.

REFERENCES

1. M. Rodbell, L. Birnbaumer, S. L. Pohl, and F. Sundby. The reaction of glucagon with its receptor: evidence for discrete regions of activity and binding in the glucagon molecule. *Proc. Natl. Acad. Sci. U.S.A.* **68**:909–913 (1971).
2. G. H. Beaven, W. B. Gratzer, and H. G. Davies. Formation and structure of gels and fibrils from glucagon. *Eur. J. Biochem.* **11**: 37–42 (1969).
3. M. J. Burke and M. A. Rougvie. Cross-β protein structures. I. Insulin fibrils. *Biochemistry* **11**:2435–2439 (1972).
4. D. K. Clodfelter, A. H. Pekar, D. M. Rebhun, K. A. Destrampe, H. A. Havel, S. R. Myers, and M. L. Brader. Effects of noncovalent self-association on the subcutaneous absorption of a therapeutic peptide. *Pharm. Res.* **15**:254–262 (1998).
5. M. Cauchy, S. D'Aoust, B. Dawson, H. Rode, and M. Hefford. Thermal stability: a means to assure tertiary structure in therapeutic proteins. *Biologicals* **30**:175–185 (2002).
6. R. J. Ellis and T. J. Pinheiro. Medicine: danger—misfolding proteins. *Nature* **416**:483–484 (2002).
7. G. G. Glenner. Amyloid deposits and amyloidosis. The beta-fibrilloses (first of two parts). *N. Engl. J. Med.* **302**:1283–1292 (1980).
8. G. G. Glenner. Amyloid deposits and amyloidosis: the beta-fibrilloses (second of two parts). *N. Engl. J. Med.* **302**:1333–1343 (1980).
9. G. Vines. Alzheimer's disease—from cause to cure? *Trends Biotechnol.* **11**:49–55 (1993).
10. G. J. Cooper, A. C. Willis, A. Clark, R. C. Turner, R. B. Sim, and K. B. Reid. Purification and characterization of a peptide from amyloid-rich pancreases of type 2 diabetic patients. *Proc. Natl. Acad. Sci. U.S.A.* **84**:8628–8632 (1987).
11. S. B. Prusiner. Prions. *Proc. Natl. Acad. Sci. U.S.A.* **95**:13363–13383 (1998).
12. E. Scherzinger, R. Lurz, M. Turmaine, L. Mangiarini, B. Hollenbach, R. Hasenbank, G. P. Bates, S. W. Davies, H. Lehrach, and E. E. Wanker. Huntingtin-encoded polyglutamine expansions form amyloid-like protein aggregates in vitro and in vivo. *Cell* **90**:549–558 (1997).
13. J. D. Sipe. Amyloidosis. *Annu. Rev. Biochem.* **61**:947–975 (1992).
14. W. G. Turnell and J. T. Finch. Binding of the dye congo red to the amyloid protein pig insulin reveals a novel homology amongst amyloid-forming peptide sequences. *J. Mol. Biol.* **227**:1205–1223 (1992).
15. I. V. Kurochkin. Amyloidogenic determinant as a substrate recognition motif of insulin-degrading enzyme. *FEBS Lett.* **427**:153–156 (1998).
16. Y. Liu and D. Schubert. Steroid hormones block amyloid fibril-induced 3-(4,5-dimethylthiazol-2- yl)-2,5-diphenyltetrazolium bromide (MTT) formazan exocytosis: relationship to neurotoxicity. *J. Neurochem.* **71**:2322–2329 (1998).
17. V. Mutt, J. E. Jorpes, and S. Magnusson. Structure of porcine secretin. The amino acid sequence. *Eur. J. Biochem.* **15**:513–519 (1970).
18. R. K. O'Dor, C. O. Parkes, and D. H. Copp. Amino acid composition of salmon calcitonin. *Can. J. Biochem.* **47**:823–825 (1969).
19. R. B. Merrifield. Solid-phase peptide synthesis. *Adv. Enzymol. Relat. Areas Mol. Biol.* **32**:221–296 (1969).
20. S. Onoue, K. Ohshima, K. Endo, T. Yajima, and K. Kashimoto. PACAP protects neuronal PC12 cells from the cytotoxicity of human prion protein fragment 106–126. *FEBS Lett.* **522**:65–70 (2002).
21. S. Onoue, K. Endo, K. Ohshima, T. Yajima, and K. Kashimoto. The neuropeptide PACAP attenuates beta-amyloid (1-42)-induced toxicity in PC12 cells. *Peptides* **23**:1471–1478 (2002).
22. W. E. Klunk, J. W. Pettegrew, and D. J. Abraham. Two simple methods for quantifying low-affinity dye-substrate binding. *J. Histochem. Cytochem.* **37**:1293–1297 (1989).
23. H. LeVine iii. Thioflavine T interaction with synthetic Alzheimer's disease beta- amyloid peptides: detection of amyloid aggregation in solution. *Protein Sci.* **2**:404–410 (1993).
24. S. Onoue, Y. Waki, Y. Nagano, S. Satoh, and K. Kashimoto. The neuromodulatory effects of VIP/PACAP on PC-12 cells are associated with their N-terminal structures. *Peptides* **22**:867–872 (2001).

25. I. Isobe, M. Michikawa, and K. Yanagisawa. Enhancement of MTT, a tetrazolium salt, exocytosis by amyloid beta- protein and chloroquine in cultured rat astrocytes. *Neurosci. Lett.* **266**:129–132 (1999).
26. N. Greenfield and G. D. Fasman. Computed circular dichroism spectra for the evaluation of protein conformation. *Biochemistry* **8**:4108–4116 (1969).
27. J. Cort, Z. Liu, G. Lee, S. M. Harris, K. S. Prickett, L. S. Gaeta, and N. H. Andersen. Beta-structure in human amylin and two designer beta-peptides: CD and NMR spectroscopic comparisons suggest soluble beta-oligomers and the absence of significant populations of beta-strand dimers. *Biochem. Biophys. Res. Commun.* **204**:1088–1095 (1994).
28. G. Forloni, N. Angeretti, R. Chiesa, E. Monzani, M. Salmona, O. Bugiani, and F. Tagliavini. Neurotoxicity of a prion protein fragment. *Nature* **362**:543–546 (1993).
29. B. Solomon, R. Koppel, E. Hanan, and T. Katzav. Monoclonal antibodies inhibit in vitro fibrillar aggregation of the Alzheimer beta-amyloid peptide. *Proc. Natl. Acad. Sci. U.S.A.* **93**:452–455 (1996).
30. W. E. Klunk, J. W. Pettegrew, and D. J. Abraham. Quantitative evaluation of congo red binding to amyloid-like proteins with a beta-pleated sheet conformation. *J. Histochem. Cytochem.* **37**: 1273–1281 (1989).
31. D. Frenkel, O. Katz, and B. Solomon. Immunization against Alzheimer's beta -amyloid plaques via EFRH phage administration. *Proc. Natl. Acad. Sci. U.S.A.* **97**:11455–11459 (2000).
32. E. Hanan, O. Goren, M. Eshkenazy, and B. Solomon. Immunomodulation of the human prion peptide 106–126 aggregation. *Biochem. Biophys. Res. Commun.* **280**:115–120 (2001).
33. K. Sasaki, S. Dockerill, D. A. Adamiak, I. J. Tickle, and T. Blundell. X-ray analysis of glucagon and its relationship to receptor binding. *Nature* **257**:751–757 (1975).
34. J. Liu, M. Bhalgat, C. Zhang, Z. Diwu, B. Hoyland, and D. H. Klaubert. Fluorescent molecular probes V: a sensitive caspase-3 substrate for fluorometric assays. *Bioorg. Med. Chem. Lett.* **9**: 3231–3236 (1999).
35. R. U. Janicke, M. L. Sprengart, M. R. Wati, and A. G. Porter. Caspase-3 is required for DNA fragmentation and morphological changes associated with apoptosis. *J. Biol. Chem.* **273**:9357–9360 (1998).
36. D. W. Nicholson, A. Ambereen, N. A. Thornberry, J. P. Vaillancourt, C. K. Ding, M. Gallant, Y. Gareau, P. R. Griffin, M. Labelle, Y. A. Lazebnik, N. A. Munday, S. M. Raju, M. E. Smulson, T. T. Yamin, V. L. Yu, and D. K. Miller. Identification and inhibition of the ICE/CED-3 protease necessary for mammalian apoptosis. *Nature* **376**:37–43 (1995).
37. E. A. Atkinson, M. Barry, A. J. Darmon, I. Shostak, P. C. Turner, R. W. Moyer, and R. C. Bleackley. Cytotoxic T lymphocyte-assisted suicide. Caspase 3 activation is primarily the result of the direct action of granzyme B. *J. Biol. Chem.* **273**:21261–21266 (1998).
38. B. L. Chen, T. Arakawa, C. F. Morris, W. C. Kenney, C. M. Wells, and C. G. Pitt. Aggregation pathway of recombinant human keratinocyte growth factor and its stabilization. *Pharm. Res.* **11**:1581–1587 (1994).
39. N. Demeester, C. Mertens, H. Caster, M. Goethals, J. Vandekerckhove, M. Rosseneu, and C. Labeur. Comparison of the aggregation properties, secondary structure and apoptotic effects of wild-type, Flemish and Dutch N-terminally truncated amyloid beta peptides. *Eur. J. Neurosci.* **13**:2015–2024 (2001).
40. K. M. Pan, M. Baldwin, J. Kguyen, M. Gasset, A. Serban, D. Groth, I. Mehlhorn, Z. Huang, R. J. Fletterick, F. E. Cohen, and S. B. Prusiner. Conversion of alpha-helices into beta-sheets features in the formation of the scrapie prion proteins. *Proc. Natl. Acad. Sci. USA* **90**:10962–10966 (1993).
41. M. Kamihira, A. Naito, S. Tuzi, A. Y. Nosaka, and H. Saito. Conformational transitions and fibrillation mechanism of human calcitonin as studied by high-resolution solid-state 13C NMR. *Protein Sci.* **9**:867–877 (2000).
42. H. J. Chae, S. W. Chae, N. H. An, J. H. Kim, C. W. Kim, S. K. Yoo, H. H. Kim, Z. H. Lee, and H. R. Kim. Cyclic-AMP inhibits nitric oxide-induced apoptosis in human osteoblast: the regulation of caspase-3, -6, -9 and the release of cytochrome c in nitric oxide-induced apoptosis by cAMP. *Biol. Pharm. Bull.* **24**:453–460 (2001).
43. J. Li, S. Yang, and T. R. Billiar. Cyclic nucleotides suppress tumor necrosis factor alpha-mediated apoptosis by inhibiting caspase activation and cytochrome c release in primary hepatocytes via a mechanism independent of Akt activation. *J. Biol. Chem.* **275**:13026–13034 (2000).